Adaptive Robust Adhesions of Barnacle-Inspired Adhesive Peptides

Evan Angelo Quimada Mondarte[1,4], Jining Wang[1,2,4], , and Jing Yu[1, 3*]

[1] School of Materials Science and Engineering, Nanyang Technological University, Singapore 639798, Singapore
[2] Singapore Membrane Technology Centre, Nanyang Environment and Water Research Institute, Nanyang Technological University, Singapore 637141, Singapore
[3] Institute for Digital Molecular Analytics and Science, Nanyang Technological University, Singapore 639798, Singapore
[4] These authors contributed equally

ABSTRACT:

The strategy of robust adhesion employed by barnacles renders them a fascinating biomimetic candidate for developing novel wet adhesives. Particularly, barnacle cement protein 19k (cp19k) has been speculated to be the key adhesive protein establishing the priming layer in the initial barnacle cement construction. In this work, we systematically studied the sequence design rationale of cp19k by designing adhesive peptides inspired from the low complexity STGA-rich and the charged segments of cp19k. Combining structure analysis and adhesion performance test, we found that cp19k-inspired adhesive peptides possess excellent disparate adhesion strategies for both hydrophilic mica and hydrophobic self-assembled monolayer surfaces. Specifically, low complexity STGA-rich segment offers great structure flexibility for surface adhesion while the hydrophobic and charged residues can contribute to the adhesion of the peptides on hydrophobic and charged surfaces. The adhesion strategy identified in this work broadens our comprehension of barnacle adhesion mechanisms and offers valuable insights for designing advanced wet adhesives with exceptional performance.

KEYWORDS: barnacle, wet adhesion, peptide, hydrogen bonds, hydrophobic interactions.

INTRODUCTION

A great challenge for artificial adhesives is to provide robust and durable adhesion in an aqueous environment. [1-3] The presence of interfacial water serves as a barrier preventing direct contact and stable bond formation between the adhesive molecules and the target surfaces. [4-7] To overcome this challenge, focus has been put on biomimicking various marine organisms such as barnacles, mussels and sandcastles worms, who have evolved fascinating wet adhesion strategies which allow them to establish strong adhesion to a diversity of underwater substrates. [8-10] The key to successful biomimicry is the understanding of functions, structures and working principles of the target organism.

Over the years, great success has been achieved on the design and fabrication of mussel-inspired wet adhesives, owing to the huge advances in the understanding of mussel adhesion mechanisms over other marine creatures. [4, 11, 12] The 3,4-dihydroxy-L-phenylalanine (Dopa)-mediated interfacial adhesion has been the most frequently adapted concept of mussel adhesion for the design of many synthetic adhesives. [9] Barnacles have also evolved effective adhesion strategy capable of attaching on almost any type of underwater substrate but not relying on post-translational modification. [8, 13]

The strong and permanent attachment of adult barnacles is achieved by a thin layer of barnacle cement (Fig. 1a) with over 90% protein content which was suggested to have no post-translational modification except for the glycosylation of cp52k (cement protein 52k). [13] Barnacle cement proteins are stored in cement glands followed by timely secretion into the circumferential edges of the baseplate and being gradually exposed to seawater environment. [14, 15] The storage glands have been reported to possess an acidic internal environment. [16] Furthermore, seawater is well-known to have an average pH value of around 8 and high ionic strength of about 0.7 M. All barnacle cement proteins would be subjected to different pH and ionic strength conditions from the secretory system to the seawater environment. This environmental shift and high salt concentration bring challenges for the adhesive proteins to offer stable and strong interfacial adhesion. Barnacle-inspired adhesives have much higher potentials for the

applications in harsh environments over mussel-inspired adhesives since Dopa, as a catecholic amino acid, is vulnerable to oxidation.[17] Unfortunately, thus far, a molecular-level understanding of barnacle adhesion mechanism remains a huge blank which significantly hindered the advancement of novel barnacle-inspired adhesives.

Previous studies have revealed the spectrum of proteins located at the adhesive interface for multiple barnacle species and named the cement proteins according to their molecular weight. [8] Specifically, *Megabalanus rosa*, the barnacle species of interest in this study possessed three major cement proteins, Mrcp52k (*Megabalanus rosa* cement protein 52k), Mrcp68k and Mrcp100k and two minor cement proteins, Mrcp19k and Mrcp20k (Fig. 1a). [13] Kei Kamino first postulated that the major cement proteins form the bulk cement while Mrcp19k and Mrcp20k are responsible for surface functions. [18] Specifically, Mrcp19k, as a priming layer, bridges the foreign substrate and the hydrophobic bulk cement, and Mrcp20k locates at the interface of the bulk cement and the calcareous baseplate, facilitating biomineralization (Fig. 1a). An early study has shown that Mrcp19k is able to strongly adsorb to various types of substrates in seawater even after washing which is one of the essential conditions for successful surface priming. [19] Meanwhile, Mrcp20k has been shown to be a calcite-specific adsorbent protein with a well-defined tertiary structure capable of regulating the calcification process to preferred crystal orientation. [20-22] It is noteworthy that cp20k only exists in barnacles with calcified baseplate and cp19k is universally present in every barnacle species, including stalked barnacles, membranous-base barnacles, and calcareous-base barnacles. [8] The utilization of cp19k as a priming layer to establish the initial adhesion with an external substrate is highly possible to be a shared strategy among all barnacle species.

The cp19k exhibits a block copolymer-like sequence arrangement with two types of alternating blocks as shown in Fig. 1b and Fig. S1. The first is an STGA-rich segment which mainly comprises of Ser, Thr, Gly and Ala, and is known as a “low complexity domain” due to the high tendency of these amino acids to form a simple and flexible structure. [23, 24] The other segment is rich in polar and charged residues (hereafter referred to as “charged segment”). Recent studies have emphasized the amyloid fiber-

forming capability of cp19k in the presence of artificial seawater. [23-25] Liang et al. tested the adhesion property of rBalcp19k (recombinant *Balanus albicostatus* cement protein 19k) before and after forming amyloid fibers on mica using atomic force microscopy (AFM). [23] However, they only tested the mineral-rBalcp19k interactions and did not cover the potential interactions of the adhesive material with the hydrophobic bulk cement. Christopher et al. first studied the amyloidogenesis property of peptides inspired from STGA-rich and charged segments of Aacp19k (*Amphibalanus amphitrite* cement protein 19k) and its homologues, highlighting the importance of molecular recognition in the barnacle adhesive curing process.[25] Instead of testing the combination of STGA-rich and charged segment, Liang et al. further tested the self-assembly properties of nine peptides inspired by each individual segment of Balcp19k. [24] Although many recent studies started to focus on the structure-function relationship of cp19k, there is yet to be a study discussing the rationale of cp19k sequence design in adhesion point of view and its capability as a priming layer.

By comparing the sequence of cp19k from five barnacle species (Fig. S1), the first domain with STGA-rich and charged segments is found to be the most representative target due to the highest sequence homology among four repetitive domains. Two adhesive peptides, Mr-AP1 (*Megabalanus rosa*-Adhesive Peptide 1; solely the STGA-rich segment) and Mr-AP1C (with charged segment), inspired from the first "STGA-rich + charged" domain of Mrcp19k (Fig. 1b and Fig. S2), are systematically studied in this work to understand the role of STGA-rich and charged segments in cp19k adhesion development.

In this work, we tested the capability of Mr-APs as a priming layer in terms of adhesion performance with respect to different solution environments using Surface Forces Apparatus (SFA). To better understand the interaction of Mr-APs with individual substrates, we also performed quantitative adsorption test by a quartz crystal microbalance (QCM) and characterized the surface morphology upon adsorption by AFM. Our results show that the presence of low complexity domain allows the formation of strong adhesive interactions with a mineral surface at low pH and low ionic strength. The addition of charged segment enhances stability in both adhesion and

conformation, providing a strategy to maintain robust adhesions to chemically different surfaces.

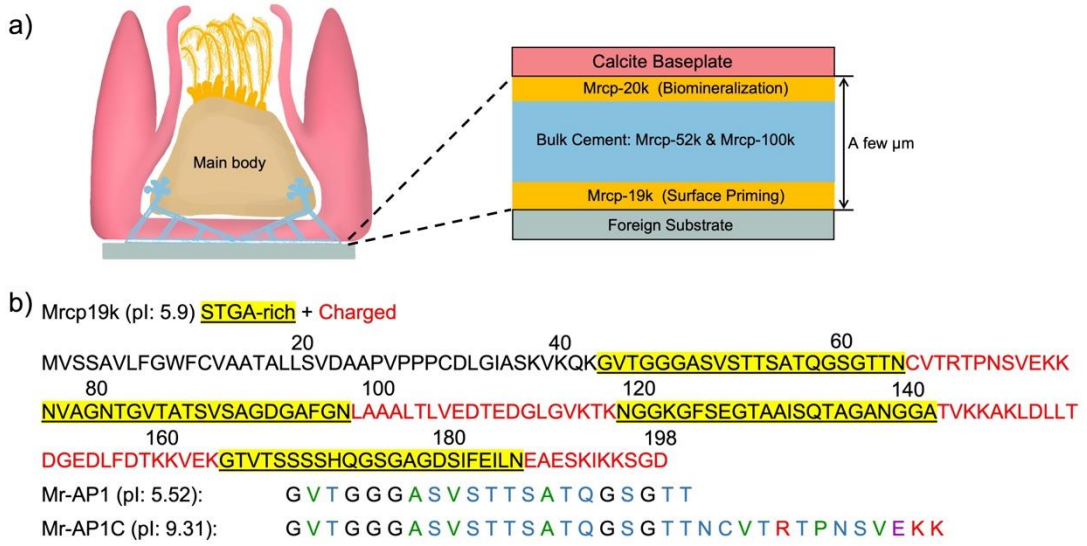

Figure 1. Adhesive peptides inspired from *Megabalanus Rosa*. a) Schematic of *Megabalanus Rosa* with highlighted distribution and function of different barnacle cement proteins. b) Sequence of Mrcp19k and two adhesive peptides inspired from first STGA-rich and charged domain of Mrcp19k.

MATERIALS AND METHODS

Materials:

Mr-AP1 and Mr-AP1C were synthesized from GenScript with over 90% purity and no modification at the termini. 2 mg/mL stock solutions of peptides were prepared in Milli-Q water, vortexed for 1min and sonicated for 20 mins before usage. Two stock buffer solutions were: 100 mM acetate buffer at pH 3.6 and 100 mM potassium phosphate buffer at pH 8. To achieve the desired NaCl concentration for each individual sample, stock buffer solutions were diluted with Milli-Q water and 5 M NaCl solution into 10 mM buffer solutions. Three salt conditions were utilized in this study: 0 mM, 100 mM and 500 mM NaCl. All chemicals used for buffer preparation were purchased from Sigma Aldrich.

Circular dichroism (CD) spectroscopy:

CD spectra of Mr-APs in various solution environment were measured using Chirascan spectropolarimeter (Model 420, AVIV Biomedical Inc.) to analyze the secondary structure of the peptides. Mr-APs were prepared into a final concentration of 1 mg/mL. All CD measurements from 190 to 260 nm were recorded with three repetitions at room temperature and with 1 nm step size and 1 nm bandwidth. The spectra were smoothed with unit converted to molar ellipticity (deg cm^2 $dmol^{-1}$).

Dynamic light scattering (DLS):

Dynamic light scattering tests were performed with Malvern Nanosizer (Malvern Panalytical, UK) to measure the hydrodynamic radius of Mr-APs at room temperature. Buffer conditions were as described in the "Materials" subsection. 500 μL of 200 μM peptide solutions were analyzed with disposable polystyrene cuvettes at room temperature. All sizes reported in this work were based on number average. Three consecutive measurements were conducted for each sample with a fixed detection angle of 90°.

Surface Forces Apparatus (SFA) Adhesion Measurement:

Adhesion strengths of Mr-APs with mica were measured with the surface forces apparatus (SFA 2000, SurForce, Santa Barbara, CA) with design and technical details reported elsewhere. [26] Freshly cleaved mica surface with 55 nm thick silver deposited at the back side, were glued to cylindrical silica disks. The distance between two surfaces was determined using the fringes of equal chromatic order (FECO) technique with white light interferometry. [27] Zero distance was denoted by the distance measured between two mica surfaces in contact for mica-mica configuration and between mica and SAM surfaces in contact for mica-SAM configuration. For each experiment, 20 μL of 0.1 mg/mL adhesive peptide solution was injected between two mica surfaces followed by a 30 min waiting time to allow adsorption and thermal equilibrium. The increment of ionic strength was achieved by carefully injecting highly concentrated calculated amount of 1-5 M NaCl solution into the peptide solution between two surfaces using a 0.5-10 μL pipette tip. Generally, the added volume ranged from 1 μL

to 3 μL. The solution was allowed to equilibrate for 30 min. Each measurement offered a normalized force-distance profile between two surfaces. The measured force (F) could be converted to the adhesion energy (E_{ad}) according to the Johnson-Kendall–Roberts (JKR) theory, $E_{ad} = F_{ad}/1.5\pi R$, where R is the effective radius of curvature of the cylindrical surface. [28]

Atomic Force Microscopy (AFM):

The morphology of the samples was obtained using a commercial AFM set-up equipped with a liquid droplet holder (Cypher S, Oxford Instruments, UK) employing the AC imaging mode. Samples were prepared by first allowing a droplet of 30 μL of 1 mg/mL peptide solution to sit on the substrate for 20 minutes followed by rinsing with the appropriate buffer. The imaging was carried out under a droplet of the buffer solution at room temperature using a cantilever with a sharp tip (nominal spring constant = 90 pN nm^{-1}, BioLever mini, Asylum Research - Oxford Instruments, USA).

Quartz crystal microbalance (QCM) adsorption test:

The adsorption test of Mr-APs was conducted using a QSense E4 instrument (Biolin Scientific AB, Sweden) on both SiO_2 and SAM-CH_3 surfaces. Silica-coated AT-cut quartz crystal sensor chips (QSX 303, Biolin Scientific AB) were used for adsorption analysis on SiO_2. To prepare SAM-modified substrates, the freshly cleaned gold-coated AT-cut quartz crystal sensor chips (QSX 301, Biolin Scientific AB) were immersed into 1 mM 1-undecanethiol ethanolic solution for 12 h. Modified substrates were thoroughly rinsed with ethanol to remove weakly attached thiol compounds and blow-dried with nitrogen gas. The sample solutions (1 mg/mL peptide concentration) were flowed into measurement chamber using a peristaltic pump (Reglo Digital MS-4/6, Ismatec, Glattbrugg, Switzerland) at a flow rate of 100 μL/min. We used QCM technique to monitor the frequency shifts (Δf) as a function of time. The adsorption data was collected using the QSoft program (Biolin Scientific AB) and processed with QSense Dfind software (Biolin Scientific AB). The data acquired at the third overtone are reported.

RESULTS AND DISCUSSION

Charged segment prevents collapse of the adhesive peptide

To first understand the structural properties of the adhesive peptides in solution before adsorption onto substrates, we used circular dichroism (CD) to characterize the secondary structure of the adhesive peptides in different solution environments. [31] We first measured the secondary structure of both peptides in solution with a pH of 3.6 as studies revealed that the MrCP-19 was stored and secreted at low pH. [16] As shown in Fig. 2a, both Mr-AP1 and Mr-AP1C are mainly comprised of random coil and beta sheet structure in a buffer condition of pH 3.6 with 100 mM NaCl. This result is consistent with major secondary structure composition of some recombinant cp19k and cp19k-inspired peptides. [19, 24, 32] The effect of changing pH and ionic strength on peptide secondary structure was also tested (Fig. S3). No significant change was observed across different pH and ionic strength values. Both Mr-APs possess consistent secondary structures compositions in response to solution condition change.

We further measured the hydrodynamic radius of the adhesive peptides using DLS. The hydrodynamic radii of both Mr-APs showed a reducing trend in response to increasing NaCl concentration (Fig. S4). NaCl was reported to be a weak kosmotrope to proteins. [33] The addition of NaCl in solution could compete with Mr-APs on interacting with water molecules. As a result, the adhesive peptides tended to shrink into smaller sizes in high concentrations of NaCl due to dehydration that leads to the enhancement of the intra-molecular interactions within the adhesive peptides. [34]

One interesting finding is that the addition of the charged segment in Mr-AP1C reduced the tendency of peptide size shrinkage compared to Mr-AP1 (Fig. S4). The slighter decrease of the hydrodynamic radius of Mr-AP1C compared to Mr-AP1 at high ionic strengths implies a better retention of the flexible and extended peptide structure with the presence of the charged segment, which showed to be of more hydrophilic nature than the STGA-rich segment (Fig. 2b). This flexibility of the adhesive protein was shown to be crucial for the reorientation of the adhesive peptide chains to establish maximum binding sites in the early stage of surface adsorption to foreign substrates. [11,

35, 36

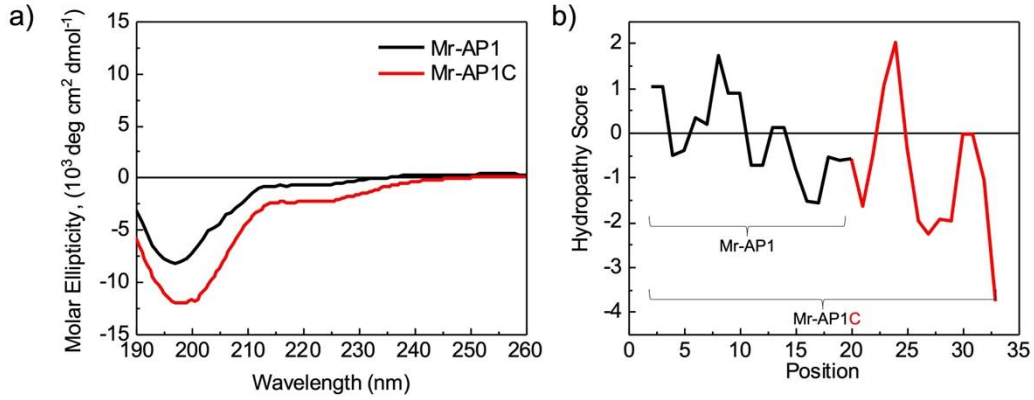

Figure 2. Characterizations of peptides in solution. a) Secondary structure of Mr-AP1 and Mr-AP1C at pH 3.6 with 100 mM NaCl. b) Hydropathy plot of Mr-AP1 and Mr-AP1C using the Kyte-Doolittle scale.

SFA revealed the strong adhesion of Mr-APs to mica

We measured the adhesion strengths of Mr-APs between two mica surfaces using the SFA technique. With no NaCl added at pH 3.6, both Mr-AP1 and Mr-AP1C exhibited adhesion on mica surfaces with adhesion energies (E_{ad}) of -1.05 ± 0.21 mJ/m^2 and -0.50 ± 0.10 mJ/m^2, respectively. (Fig. 3a-b). The SFA force profile also showed a hard wall at ~ 0.5 nm and ~ 3 nm for Mr-AP1 and Mr-AP1C, respectively, which is consistent with the peptide size distributions from the DLS results (Figure S4). When the ionic strength was increased with a fixed pH of 3.6, the adhesion force of Mr-AP1 further diminished with the increase of the hard-wall distance (Fig. 3c). However, with the addition of the charged segment, Mr-AP1C showed comparable adhesions (E_{ad} = -0.50 ± 0.10, -0.50 ± 0.06, and -0.51 ± 0.02 mJ/m^2 for 0, 100 and 500 mM NaCl, respectively) and fairly consistent hard-wall distance at ~ 3 nm with increasing ionic strength at pH 3.6 (Fig. 3d).

The hard wall at approximately less than 3 nm in the majority of the force profiles suggests that the adhesive peptides form a monomolecular layer of peptide oligomers in between two mica surfaces and thus, we can attribute the adhesion strengths to the peptide-surface interactions. When exposed to environments with high NaCl

concentration, Mr-AP1 shrunk due to dehydration, (Fig. S4a-b) which led to a reduced accessibility of residues capable of establishing stable hydrogen bonds with the mica surfaces. Therefore, with high NaCl concentration, the adhesion of Mr-AP1 with mica surface was weakened. The increase of the hard-wall distance at high salt concentration also depicted the occurrence of peptide dehydration as peptides (especially proteins) typically agglomerate when dehydrated. In comparison, the additional charged segment of MrAP1C provide resistance to salt-induced shrinkage due to a stronger hydrophilic character (Fig. S4c-d and Fig. 2b). Moreover, the positive charges such as Lys and Arg of the charged segment could facilitate the adhesion of the peptide to mica surface by electrostatically binding to the negatively charged mica surfaces. [37] No adhesion was measured for both Mr-APs in all salt concentrations at the buffer condition of pH 8 (Figure 3 a, b and Fig. S5). A noteworthy finding is the significant increase in the hard-wall distance with repulsion range to up to 45 nm at increased salt concentration for MrAP1 at pH 8 (Fig S5). This value is far from the size of the peptide as obtained by DLS, thus indicating aggregation of the peptides in this pH condition. We discuss about this observation later at the next section (see Surface adsorption of Mr-APs) with the substantiation from QCM and AFM results.

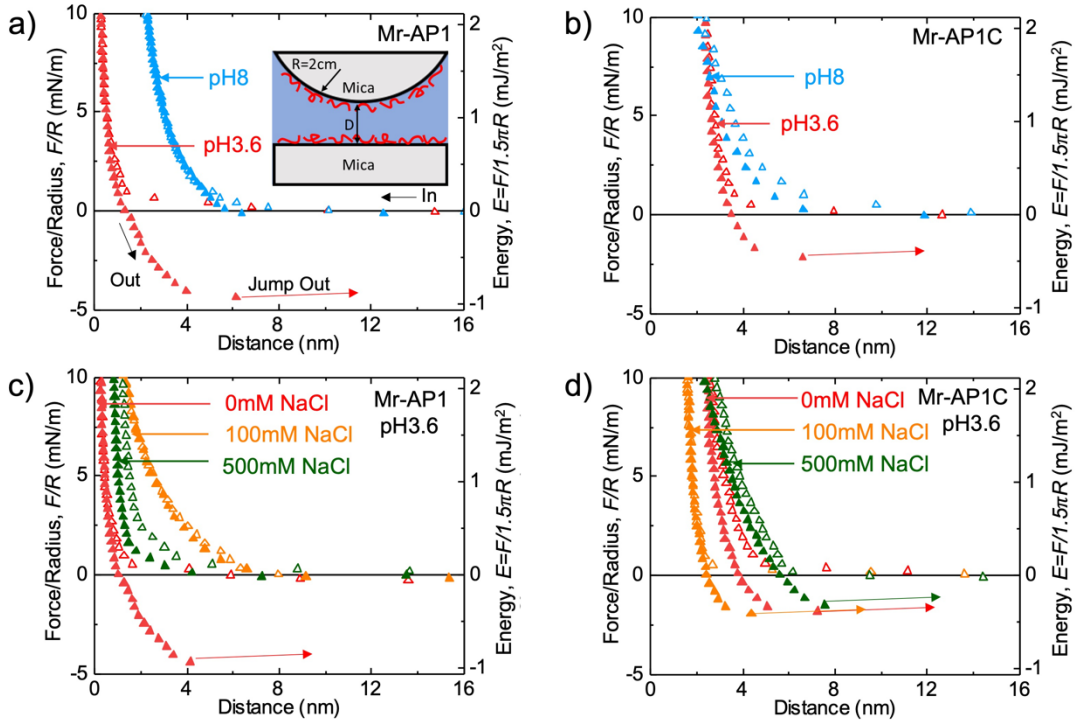

Figure 3. Adhesion measurement result: mica and mica. a) Mr-AP1 at pH 3.6 and pH 8 with no NaCl. b) Mr-AP1C at pH 3.6 and pH 8 with no NaCl. c) Mr-AP1 at pH 3.6 with 0, 100 mM, 500 mM NaCl. d) Mr-AP1C at pH 3.6 with 0, 100 mM, 500 mM NaCl.

Surface adsorption of Mr-APs

We also performed adsorption test by QCM on SiO_2 sensors, which has a chemical structure close to mica. Additionally, we included SAM-CH_3-modified gold sensors to test the adsorption of the peptides on a hydrophobic surface (Fig. 4). In QCM measurements, the amount of adsorbed material per area is proportional to the frequency shifts monitored by the sensor (Fig. 4a). [38] At pHs 3.6 and 8 in all salt concentrations, nearly all Mr-AP1 molecules were washed away by buffer which led to almost zero frequency shifts. Meanwhile, Mr-AP1C presented higher frequency shifts relative to Mr-AP1 across all pH conditions and ionic strength conditions (Fig. 4b) (the frequency shift values compared in this work are absolute values). The consistent almost zero adsorption of MrAP1 seems to contradict with the SFA force profile in which an adhesion force is observed at pH 3.6 with no salt added. Aggregations were even observed upon increasing the salt concentration as depicted by the increase in the range of repulsion (Fig. 3c). Moreover, longer-ranged repulsions (25 nm and 45 nm for 100 mM and 500 mM, respectively) appeared at pH 8, indicating substantial aggregation (Fig. 4b and Fig. S5a). It is likely that the thick aggregation of peptides in these solution conditions were weakly bound to the surface and can be easily washed away by the rinsing process performed in the QCM experiments. Another possible explanation is the influence of the additional metal ions at the mineral mica surface, which are not present in a pure silica surface. The most accurate comparison would be achieved by employing a mica-modified QCM sensor surface which is still a non-established protocol that poses several complications in measurements and analysis. Nevertheless, corresponding to the SFA results, Mr-AP1C showed to adsorb more on a hydrophilic SiO_2 surface than Mr-AP1. Mr-AP1C exhibited the highest frequency shift when no NaCl is added for both pH values. Less frequency shifts were displayed in

higher salt concentrations. Counterions from the saline solution might have screened the charged residues consequentially making it more difficult for the peptides to approach the surface and establish stable H-bonds. This is different from SFA experiments where the two mica surfaces are brought to contact, bringing the peptides closer to the surfaces and facilitating the formation of the short-ranged H-bonds. However, the frequency shifts at pH 8 for Mr-AP1C are consistent and close to the values at pH 3.6 showing stability of adsorption in low and high pH conditions (Fig. 4b). It is noteworthy that at high pH, no to weak adhesion strengths were found in the SFA measurements (Fig. S5b), which implies that although MrAP1C stably adsorb on mica, a bridging interaction is difficult to establish for two opposing mica surfaces. One mica surface can predominantly accommodate the H-bond forming residues, which appreciably decreases the binding sites for another mica surface. Similar phenomenon has been observed for short adhesive peptides derived from mussel adhesive proteins. [39]

For gold sensors functionalized with SAM-CH_3, both Mr-APs gave high frequency shift values across the different solution environment tested (Fig. 4c). We attribute these high peptide adsorptions to the nonpolar residues of the STGA-rich segment, which are responsible in forming hydrophobic interaction with the methyl-terminated SAM surface. Mr-AP1C was observed to possess higher frequency shift values compared to Mr-AP1. The difference could be due to the presence of three additional nonpolar amino acid residues in the charged segment (two Val and one Pro). At pH 3.6, the mean value of frequency shift for Mr-AP1C is consistently high in all salt concentrations, indicating higher stability in terms of adhesion to SAM-CH_3 compared to Mr-AP1. At pH 8, high frequency shifts were also observed but with a quite decrease at 500 mM salt. Although the high concentration of salt affected the adsorption of the peptide in a slightly basic condition, the presence of the charged segment of Mr-AP1C still proves to aid in reducing this effect of salt-induced peptide shrinkage that disables some residues to access surfaces for adhesion.

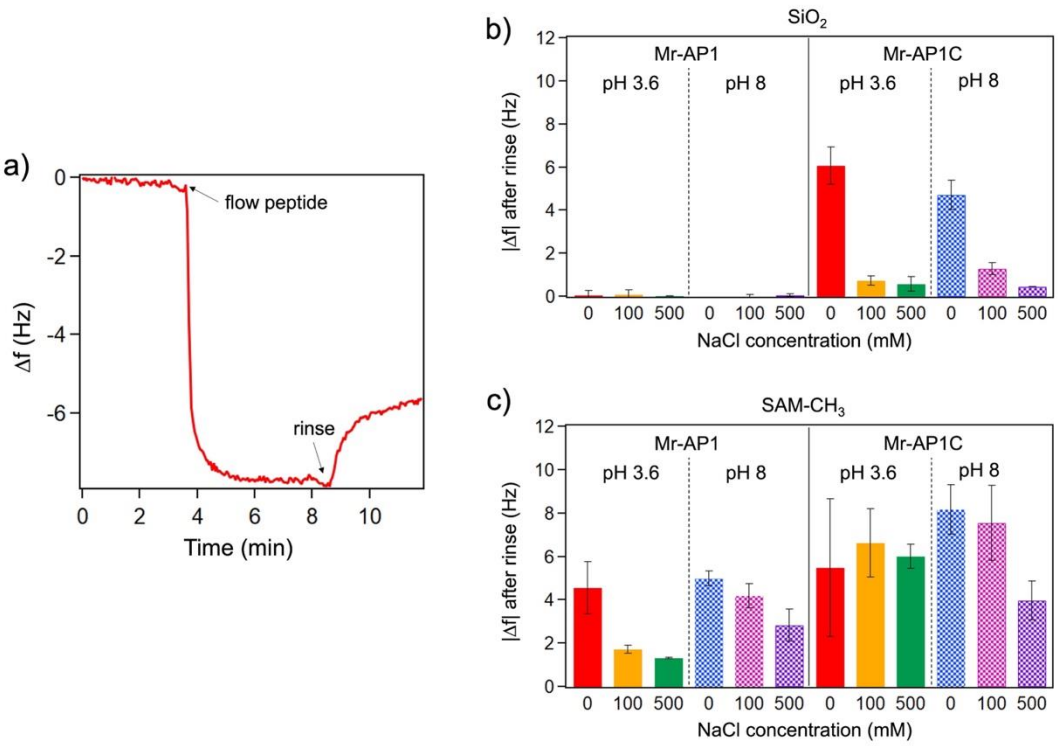

Figure 4. Adsorption of adhesive peptides on SiO_2 monitored by QCM sensors. a) A representative frequency shift (Δf) profile as a function of time for peptide adsorption taken for Mr-AP1 at pH 3.6 with no added NaCl. b-c) The absolute values of final frequency shifts of Mr-APs after rinsing with buffer on SiO_2 (middle) and on SAM-CH_3 (right) for pH 3.6 and pH 8 with 0, 100, and 500 mM NaCl.

We further used AFM with a liquid droplet holder to image the adsorbed peptides on mica in different solution environments as shown in Fig. 5 and Fig. S6. Both Mr-AP1 and Mr-AP1C produced small and thin adhesive patches (less than 7 nm in thickness) uniformly distributed on mica surface at pH 3.6. When the NaCl concentration was increased, the number of patches became less and less but the size of patches remained comparable. AFM images substantially agrees with the QCM and SFA results showing less susceptibility of Mr-AP1C to varying ionic strengths compared to Mr-AP1. Similar comparison can be drawn from the images at pH 8 (Fig. S6), although some tiny patches can be identified for pH 8 at higher salt concentrations for Mr-AP1. QCM and SFA results have revealed that these patches are weakly adsorbed on the surface. A more rigorous rinsing process, similar to that in QCM tests, could have washed off these physisorbed patches. Furthermore, at pH 8 with 500 mM NaCl, Mr-AP1C exhibited a fibril-like morphology (Fig. S6f). This is an interesting

result which could not be deciphered from the force profiles in SFA measurements and the acoustic sensing by QCM. Nevertheless, it is consistent with the previously proposed self-assembly mechanism of barnacle cement where the seawater condition including both a basic pH and high salt concentration could serve as a trigger to stimulate the fiber formation of barnacle cement proteins. [23-25, 40]

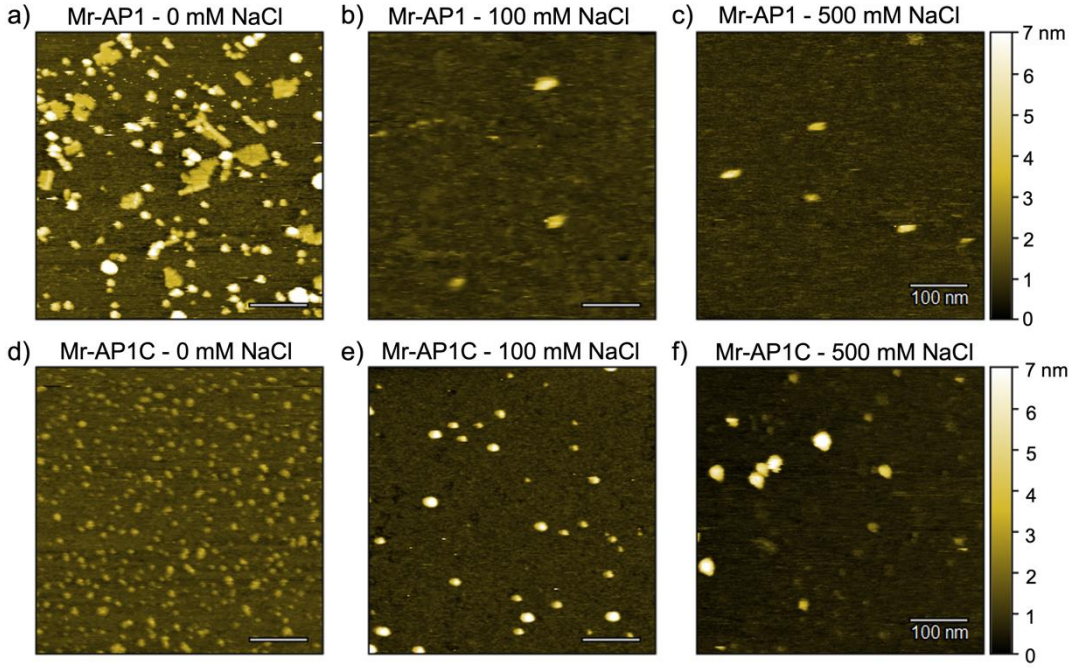

Figure 5. Morphology of adsorbed peptides on mica at pH 3.6. Mr-AP1 (top images) adsorbed on mica surface at pH 3.6 in a) 0 mM, b) 100 mM, and c) 500 mM NaCl buffer. Mr-AP1C (bottom images) adsorbed on mica surface at pH 3.6 in d) 0 mM, e) 100 mM, and f) 500 mM NaCl buffer.

Rationalizing the peptide sequence design for adaptive robust adhesions

From the SFA adhesion measurement, Mr-AP1C showed to establish stronger adhesion than Mr-AP1 in all environment conditions used in this study. (Fig. 3). QCM results further substantiated the capability of Mr-AP1C in forming stable adsorption on either hydrophilic SiO_2 or hydrophobic SAM-CH_3 (Fig. 4). These results indicate that Mr-AP1C which contains both the flexible STGA-rich segment and the additional charged segment can adapt to environment conditions to establish robust adhesions to different kinds of surfaces. When the peptides adsorb on a mineral surface, the low complexity domain aids in forming patches (Fig. 5) stabilized by multiple hydrogen bonds between the polar amino acid residues (like Ser and Thr) and the mica surface.

Moreover, the hydrated flexible structure permits the high utilization rate of binding sites. The positive charges from Lys and Arg provided additional electrostatic attraction with the mineral surface. Moreover, the stronger hydrophilicity of the charged segment endows Mr-AP1C resistance to salt-induced dehydration. On the other hand, when exposed to a hydrophobic surface (SAM-CH_3), the nonpolar residues are able to form strong hydrophobic interaction with the surface (Fig. 6). As a result, Mr-AP1C exhibited excellent adhesions on surfaces with disparate properties shedding light to the barnacle's strategy for robust heterogenous adhesion. This characteristic makes Mr-AP1C perfect candidate for versatile wet adhesives.

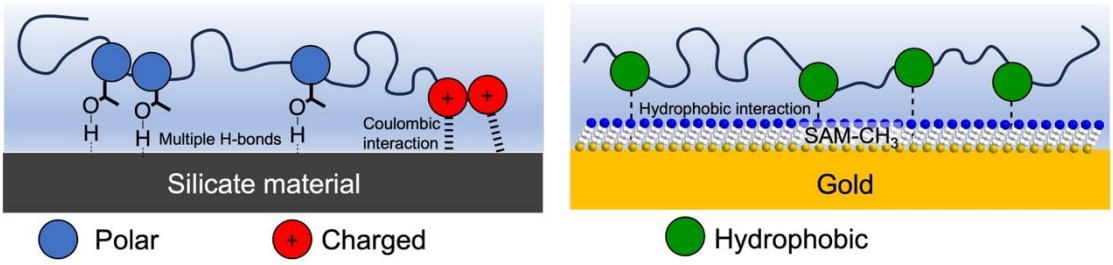

Figure 6. Schematic representation of the Mr-AP1C adhesions on a silicate material (left) and SAM-CH_3 (right).

CONCLUSIONS

The cp19k-inspired peptide adhesives have excellent heterogenous adhesion property, which facilitate them to form strong adhesive interactions with both a mineral substrate via multiple hydrogen bonds and a bulk-cement-like interface via hydrophobic interaction (Fig. 6). By comparing the sequences of cp19k homologs from several barnacle species, we designed two Mrcp19k-inspired adhesive peptides (Mr-AP1 and Mr-AP1C) and tested the role of low complexity domain and charged segments on adhesion for the first time. Our results suggest that the low complexity domain possesses great structure flexibility and allows the adhesive molecules to establish the maximum H-bond interactions with the mineral substrate and form adhesive patches at low pH and low ionic strength. For a hydrophobic surface, the

nonpolar amino acids are responsible in establishing strong hydrophobic interaction with the hydrophobic interface of bulk cement. More importantly, the charged segment in Mr-AP1C plays a key role in establishing robust and stable adhesion by 1) maintaining flexibility of the hydrated structure under high NaCl concentration in seawater, and 2) enhancing the adhesion with additional positive charges and hydrophobic residues. Notably, this work first illustrates that both STGA-rich and charged segments are critical in priming an underwater substrate at the early stage of adult barnacle cement construction. With great simplicity and high environmental tolerance, the heterogenous adhesion strategy of barnacles owns great potential to inspire novel underwater adhesives with broad applicability among disparate surfaces.

ASSOCIATED CONTENT

Supporting Information

Cp19k sequence homology from different barnacle species; mass spectroscopy results of Mr-APs; CD spectra and DLS results in different NaCl concentrations and pH values; adhesion measurement results at pH 8, and AFM images at pH 8

AUTHOR INFORMATION

Corresponding Author

Jing Yu - School of Materials Science and Engineering, Nanyang Technological University, 639798, Singapore; orcid.org/0000-0002-4288-951X
Email: yujing@ntu.edu.sg

Author

Jining Wang - School of Materials Science and Engineering, Nanyang Technological University, 639798, Singapore; Singapore Membrane Technology Centre, Nanyang

Environment and Water Research Institute, Nanyang Technological University, Singapore 637141, Singapore; orcid.org/0000-0002-1209-4855

Evan Angelo Quimada Mondarte - School of Materials Science and Engineering, Nanyang Technological University, 639798, Singapore; orcid.org/0000-0003-1651-9512

Author Contributions

[4]These authors contributed equally.

Notes

The authors declare no competing financial interest.

ACKNOWLEDGMENT

This work is supported by the Singapore National Research Fellowship (NRF-NRFF11-2019-0004) and the Singapore Ministry of Education (MOE) Tier 2 Grant (MOE-T2EP30220-0006).

REFERENCES:

1. Pocius, A.V. *Adhesion and Adhesives Technology: An Introduction*; Carl Hanser Verlag GmbH Co KG, 2021.
2. Cloete, W.E.; W.W. Focke. Fast Underwater Bonding to Polycarbonate Using Photoinitiated Cyanoacrylate. *International journal of adhesion and adhesives* 2010, 30 (4), 208-213.
3. Frantzis, P. Durability of Adhesive Joints Made Underwater. *Journal of materials in civil engineering* 2008, 20 (10), 635-639.
4. Lee, B.P.; P.B. Messersmith; J.N. Israelachvili; J.H. Waite. Mussel-Inspired Adhesives and Coatings. *Annual review of materials research* 2011, 41, 99.
5. Stewart, R.J.; T.C. Ransom; V. Hlady. Natural Underwater Adhesives. *Journal of Polymer Science Part B: Polymer Physics* 2011, 49 (11), 757-771.
6. Mondarte, E.A.Q.; E.M.M. Zamarripa; R. Chang; F. Wang; S. Song; H. Tahara; T. Hayashi. Interphase Protein Layers Formed on Self-Assembled Monolayers in Crowded Biological Environments: Analysis by Surface Force and Quartz Crystal Microbalance Measurements. *Langmuir* 2022, 38 (4), 1324-1333. DOI: 10.1021/acs.langmuir.1c02312 From NLM.

7. Tanaka, M.; T. Hayashi; S. Morita. The Roles of Water Molecules at the Biointerface of Medical Polymers. *Polymer Journal* 2013, 45 (7), 701-710. DOI: 10.1038/pj.2012.229.
8. Liang, C.; J. Strickland; Z. Ye; W. Wu; B. Hu; D. Rittschof. Biochemistry of Barnacle Adhesion: An Updated Review. *Frontiers in Marine Science* 2019, 6, 565.
9. Waite, J.H. Mussel Adhesion–Essential Footwork. *Journal of Experimental Biology* 2017, 220 (4), 517-530.
10. Stewart, R.J.; C.S. Wang; I.T. Song; J.P. Jones. The Role of Coacervation and Phase Transitions in the Sandcastle Worm Adhesive System. *Advances in colloid and interface science* 2017, 239, 88-96.
11. Bandara, N.; H. Zeng; J. Wu. Marine Mussel Adhesion: Biochemistry, Mechanisms, and Biomimetics. *Journal of adhesion science and technology* 2013, 27 (18-19), 2139-2162.
12. Guo, Q.; J. Chen; J. Wang; H. Zeng; J. Yu. Recent Progress in Synthesis and Application of Mussel-Inspired Adhesives. *Nanoscale* 2020, 12 (3), 1307-1324.
13. Kamino, K. Barnacle Underwater Attachment. In Biological Adhesives, Springer, 2016; pp 153-176.
14. Burden, D.K.; C.M. Spillmann; R.K. Everett; D.E. Barlow; B. Orihuela; J.R. Deschamps; K.P. Fears; D. Rittschof; K.J. Wahl. Growth and Development of the Barnacle Amphibalanus Amphitrite: Time and Spatially Resolved Structure and Chemistry of the Base Plate. *Biofouling* 2014, 30 (7), 799-812.
15. Fears, K.P.; B. Orihuela; D. Rittschof; K.J. Wahl. Acorn Barnacles Secrete Phase‐Separating Fluid to Clear Surfaces Ahead of Cement Deposition. *Advanced Science* 2018, 5 (6), 1700762.
16. Power, A.M.; W. Klepal; V. Zheden; J. Jonker; P. McEvilly; J.v. Byern. Mechanisms of Adhesion in Adult Barnacles. In Biological Adhesive Systems, Springer, 2010; pp 153-168.
17. Barrett, D.G.; D.E. Fullenkamp; L. He; N. Holten-Andersen; K.Y.C. Lee; P.B. Messersmith. Ph-Based Regulation of Hydrogel Mechanical Properties through Mussel-Inspired Chemistry and Processing. *Advanced Functional Materials* 2013, 23 (9), 1111-1119. DOI: https://doi.org/10.1002/adfm.201201922.
18. Kamino, K. Underwater Adhesive of Marine Organisms as the Vital Link between Biological Science and Material Science. *Marine Biotechnology* 2008, 10 (2), 111-121.
19. Urushida, Y.; M. Nakano; S. Matsuda; N. Inoue; S. Kanai; N. Kitamura; T. Nishino; K. Kamino. Identification and Functional Characterization of a Novel Barnacle Cement Protein. *The FEBS journal* 2007, 274 (16), 4336-4346.
20. Mori, Y.; Y. Urushida; M. Nakano; S. Uchiyama; K. Kamino. Calcite‐Specific Coupling Protein in Barnacle Underwater Cement. *The FEBS Journal* 2007, 274 (24), 6436-6446.
21. Kumar, A.; H. Mohanram; J. Li; H. Le Ferrand; C.S. Verma; A. Miserez. Disorder–Order Interplay of a Barnacle Cement Protein Triggered by Interactions with Calcium and Carbonate Ions: A Molecular Dynamics Study. *Chemistry of Materials* 2020, 32 (20), 8845-8859.
22. Mohanram, H.; A. Kumar; C.S. Verma; K. Pervushin; A. Miserez. Three-Dimensional Structure of Megabalanus Rosa Cement Protein 20 Revealed by Multi-Dimensional Nmr and Molecular Dynamics Simulations. *Philosophical Transactions of the Royal Society B* 2019, 374 (1784), 20190198.
23. Liang, C.; Z. Ye; B. Xue; L. Zeng; W. Wu; C. Zhong; Y. Cao; B. Hu; P.B. Messersmith. Self-Assembled Nanofibers for Strong Underwater Adhesion: The Trick of Barnacles. *ACS applied materials & interfaces* 2018, 10 (30), 25017-25025.

24. Liang, C.; X. Bi; K. Gan; J. Wu; G. He; B. Xue; Z. Ye; Y. Cao; B. Hu. Short Peptides Derived from a Block Copolymer-Like Barnacle Cement Protein Self-Assembled into Diverse Supramolecular Structures. *Biomacromolecules* 2022, 2019-2030.
25. So, C.R.; E.A. Yates; L.A. Estrella; K.P. Fears; A.M. Schenck; C.M. Yip; K.J. Wahl. Molecular Recognition of Structures Is Key in the Polymerization of Patterned Barnacle Adhesive Sequences. *ACS nano* 2019, 13 (5), 5172-5183.
26. Israelachvili, J.; Y. Min; M. Akbulut; A. Alig; G. Carver; W. Greene; K. Kristiansen; E. Meyer; N. Pesika; K. Rosenberg. Recent Advances in the Surface Forces Apparatus (Sfa) Technique. *Reports on Progress in Physics* 2010, 73 (3), 036601.
27. Connor, J.N.; R.G. Horn. Extending the Surface Force Apparatus Capabilities by Using White Light Interferometry in Reflection. *Review of scientific instruments* 2003, 74 (11), 4601-4606.
28. Israelachvili, J.N. *Intermolecular and Surface Forces*; Academic press, 2011, 442-448.
29. Hegner, M.; P. Wagner; G. Semenza. Ultralarge Atomically Flat Template-Stripped Au Surfaces for Scanning Probe Microscopy. *Surface Science* 1993, 291 (1-2), 39-46.
30. Chai, L.; J. Klein. Large Area, Molecularly Smooth (0.2 Nm Rms) Gold Films for Surface Forces and Other Studies. *Langmuir* 2007, 23 (14), 7777-7783.
31. Greenfield, N.J. Using Circular Dichroism Spectra to Estimate Protein Secondary Structure. *Nature protocols* 2006, 1 (6), 2876-2890.
32. Barnes, C.; K. Fears; D. Leary; J. Scancella; Z. Wang; J. Liu; B. Orihuela; D. Rittschof; C. Spillmann; K. Wahl. Sequence Basis of Barnacle Cement Nanostructure Is Defined by Proteins with Silk Homology. *Scientific Reports (Nature Publishing Group)* 2016, (36219).
33. Collins, K.D. Charge Density-Dependent Strength of Hydration and Biological Structure. *Biophysical journal* 1997, 72 (1), 65-76.
34. Queiroz, J.; C. Tomaz; J. Cabral. Hydrophobic Interaction Chromatography of Proteins. *Journal of biotechnology* 2001, 87 (2), 143-159.
35. DeBenedictis, E.P.; J. Liu; S. Keten. Adhesion Mechanisms of Curli Subunit Csga to Abiotic Surfaces. *Science advances* 2016, 2 (11), e1600998.
36. Petrone, L.; A. Kumar; C.N. Sutanto; N.J. Patil; S. Kannan; A. Palaniappan; S. Amini; B. Zappone; C. Verma; A. Miserez. Mussel Adhesion Is Dictated by Time-Regulated Secretion and Molecular Conformation of Mussel Adhesive Proteins. *Nature communications* 2015, 6 (1), 1-12.
37. Maier, G.P.; M.V. Rapp; J.H. Waite; J.N. Israelachvili; A. Butler. Adaptive Synergy between Catechol and Lysine Promotes Wet Adhesion by Surface Salt Displacement. *Science* 2015, 349 (6248), 628-632.
38. Reviakine, I.; D. Johannsmann; R.P. Richter. Hearing What You Cannot See and Visualizing What You Hear: Interpreting Quartz Crystal Microbalance Data from Solvated Interfaces. *Anal Chem* 2011, 83 (23), 8838-48. DOI: 10.1021/ac201778h From NLM.
39. Wei, W.; J. Yu; M.A. Gebbie; Y. Tan; N.R. Martinez Rodriguez; J.N. Israelachvili; J.H. Waite. Bridging Adhesion of Mussel-Inspired Peptides: Role of Charge, Chain Length, and Surface Type. *Langmuir* 2015, 31 (3), 1105-1112.
40. Nakano, M.; K. Kamino. Amyloid-Like Conformation and Interaction for the Self-Assembly in Barnacle Underwater Cement. *Biochemistry* 2015, 54 (3), 826-835.
41. Grimsley, G.R.; J.M. Scholtz; C.N. Pace. A Summary of the Measured Pk Values of the Ionizable Groups in Folded Proteins. *Protein Science* 2009, 18 (1), 247-251.
42. Heath, M.D.; B. Henderson; S. Perkin. Ion-Specific Effects on the Interaction between

Fibronectin and Negatively Charged Mica Surfaces. *Langmuir* 2010, 26 (8), 5304-5308.